

ARMY RESEARCH LABORATORY



# Dynamic Mechanical Analysis of E-Beam and Thermally Curable IPN Thermosets

by Robert E. Jensen, Giuseppe R. Palmese, and  
Steven H. McKnight

ARL-TR-2698

March 2002

Approved for public release; distribution is unlimited.

20020402 172

The findings in this report are not to be construed as an official Department of the Army position unless so designated by other authorized documents.

Citation of manufacturer's or trade names does not constitute an official endorsement or approval of the use thereof.

Destroy this report when it is no longer needed. Do not return it to the originator.

# Army Research Laboratory

Aberdeen Proving Ground, MD 21005-5069

---

ARL-TR-2698

March 2002

---

## Dynamic Mechanical Analysis of E-Beam and Thermally Curable IPN Thermosets

Robert E. Jensen and Steven H. McKnight

Weapons and Materials Research Directorate, ARL

Giuseppe R. Palmese

Drexel University

---

---

## Abstract

---

Interpenetrating polymer network (IPN) materials possess unique properties that can be exploited for multicomponent composite armor systems, including toughness and thermal stability. E-beam curing of composites and adhesives offers advantages, such as reduced cure shrinkages, over traditional autoclave processing by curing multiple resins through the thickness for thick-section composites in a single step. Because of the complexity and thickness of composite integral armor structures, e-beam curing is an attractive processing method for Future Combat System applications, and the development of these new resins permits this approach. This research seeks to discern the differences in viscoelastic behavior between traditional thermal and e-beam curing in IPN resins, as these viscoelastic characteristics may prove important for composite integral armor applications.

---

## Acknowledgments

---

This research was supported in part by an appointment to the Research Participation Program at the U.S. Army Research Laboratory (ARL) administered by the Oak Ridge Institute for Science and Education through an interagency agreement between the U.S. Department of Energy and ARL. The authors also wish to acknowledge the ARL Composite Materials Research Materials Center of Excellence and the University of Delaware Center for Composite Materials whose participation through the joint contract DAAL01-96-2-0048 provided additional support.

INTENTIONALLY LEFT BLANK.

---

## Contents

---

Acknowledgments	iii
List of Figures	vii
List of Tables	ix
1. Introduction	1
2. Materials	1
3. Experimental	2
4. Results and Discussion	3
5. References	17
List of Acronyms and Abbreviations	21
Distribution List	23
Report Documentation Page	29

INTENTIONALLY LEFT BLANK.

---

## List of Figures

---

Figure 1. IPN resin constituents. ....	2
Figure 2. Storage modulus plots for thermal-cured IPNs.....	4
Figure 3. Storage modulus plots for e-beam-cured IPNs. ....	4
Figure 4. Loss modulus plots for thermal-cured IPNs.....	5
Figure 5. Loss modulus plots for e-beam-cured IPNs.....	5
Figure 6. Loss tangent plots for thermal-cured IPNs. ....	6
Figure 7. Loss tangent plots for e-beam-cured IPNs. ....	6
Figure 8. Loss modulus frequency sweep measurements of e-beam-cured 1-3 sample.....	9
Figure 9. Loss tangent frequency sweep measurements of e-beam-cured 1-3 sample.....	10
Figure 10. Loss modulus frequency sweep measurements of thermal-cured 1-3 sample.....	11
Figure 11. Loss tangent frequency sweep measurements of thermal-cured 1-3 sample.....	11
Figure 12. Loss modulus $E''$ master curves and KWW fits for thermal-cured samples.....	13
Figure 13. $E''$ master curves and KWW fits for e-beam-cured samples.....	14
Figure 14. Shift factor plots for thermal-cured IPNs. ....	15
Figure 15. Shift factor plots for e-beam-cured IPNs. ....	16

INTENTIONALLY LEFT BLANK.

---

## List of Tables

---

Table 1. Viscoelastic parameters derived from fits of master curves.....	15
--	----

INTENTIONALLY LEFT BLANK.

---

## 1. Introduction

---

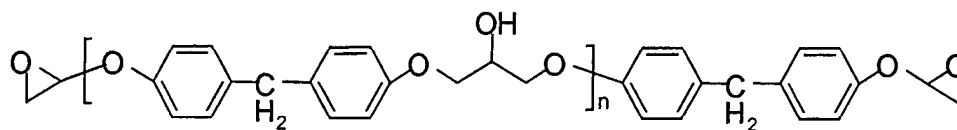
Polymer composites and adhesively bonded hybrid composite structures (e.g., composite-ceramic integral armor) are promising candidates for ultralightweight structural armor for Future Combat Systems (FCS). The development of composite resins for low-cost processing with improved properties will speed insertion of lightweight materials into FCS platforms. The processing and performance shortfalls in suitable resins may be addressed through exploitation of new electron beam (e-beam) curable systems including recently developed interpenetrating polymer network (IPN) materials. IPNs are polymers that are formed from the independent polymerization of two or more distinct networks, which results in unique molecular and physical microstructures offering improved properties [1]. The IPN materials are demonstrated to possess unique properties that can be exploited for multicomponent composite armor systems, including toughness and thermal stability. E-beam curing of composites and adhesives offers advantages, such as reduced cure shrinkages, over traditional autoclave processing by curing multiple resins through the thickness of thick-section composites in a single step. Because of the complexity and thickness of composite integral armor structures, e-beam curing is an attractive processing method for FCS applications and the development of these new resins permit this approach. This research seeks to discern the differences in viscoelastic behavior between traditional thermal and e-beam curing in IPN resins, as these viscoelastic characteristics may prove important for composite integral armor applications.

---

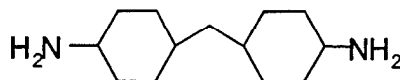
## 2. Materials

---

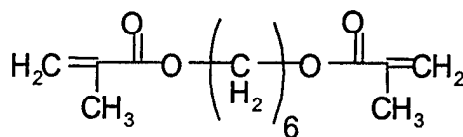
Dalal and Palmese previously developed the IPN formulation and cure routes [2]. The IPN formulation consisted of an epoxy network—diglycidyl ether of bisphenol F (DGEBF) (EEW = 170 g/mol) cured with bis(p-aminocyclohexyl) methane (EEW = 52.5 g/mol)—coupled to a free radical methacrylate network (1,6-hexanediol dimethacrylate [HDDMA]). The HDDMA free radical crosslinking reaction mechanism was initiated either via e-beam or thermal using the organic peroxide initiator 2,5-dimethyl-2,5-di-(t-butylperoxy) hexane. To couple the epoxy and methacryl networks together, a partial esterification reaction was used to convert an epoxy functionality of triphenylolmethane triglycidyl ether (TMTE) (EEW = 162 g/mol) to a methacryl functionality following the procedure outlined previously [2]. This 33% methacrylated TMTE, along with the other constituents, is illustrated in Figure 1.



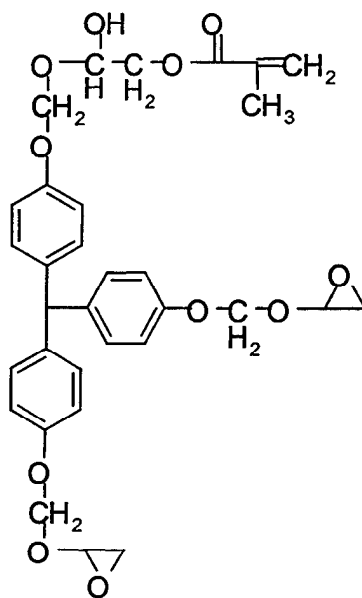
diglycidyl ether of bisphenol F (DGEBF) Epoxy



Bis(p-aminocyclohexyl) methane (PACM)



1,6-hexanediol dimethacrylate (HDDMA)



33% methacrylated triphenylmethane triglycidyl ether (33% TMTE)

Figure 1. IPN resin constituents.

---

### 3. Experimental

---

To study the influence of coupling between the DGEBF and HDDMA networks by the 33% TMTE the molar ratio of DGEBF to 33% TMTE was systematically varied from 4 mols of DGEBF to 0 mols of 33% TMTE (4-0 samples) through

0 mols of DGEBF to 4 mols of 33% TMTE (0–4 samples). Intermediate molar ratios of DGEBF:33% TMTE (3:1, 2:2, and 1:3) were also examined. The PACM concentration was always maintained at stoichiometry with respect to the DGEBF and 33% TMTE epoxy resins. The weight fraction of DGEBF and TMTE to HDDMA was maintained at a constant ratio of 0.70 to 0.30.

Two routes of curing the IPNs were pursued. The thermal cure conditions consisted of an initial cure at 70 °C for 3 hr, followed by cure at 140 °C for 2 hr, and a final post-cure at 250 °C for 1 hr. The two-stage curing schedule was selected to strictly control the formation of the epoxy-amine templated network. Previous research has shown that the Michael's addition side-reaction between the methacrylates and the PACM is minimal at 70 °C [2]. Therefore, the epoxy-amine stoichiometry is maintained. The e-beam cure route consisted of initial cure at 70 °C for 3 hr, followed by e-beam cure at a radiation dose of 20 Mrad, and a final post-cure at 250 °C for 1 hr.

Dynamic mechanical analysis (DMA) was performed using a TA Instruments 2980 DMA in the dual cantilever-bending mode. The samples were tested using a 20-mm frame and oscillatory displacement amplitude of 7.5  $\mu\text{m}$ . The displacement amplitude was verified to ensure linear viscoelastic response by deriving corresponding stress-strain curves. The typical sample's width and thickness were approximately 12 mm  $\times$  2 mm, respectively. Constant heating rate experiments were carried out at 2.0 °C/min, with a frequency of 1 Hz from 50° to 275 °C. Master curves were constructed from data obtained from multiple frequency sweeps, which were measured over three decades of frequency, ranging from 0.1 to 30 Hz in 3 °C isothermal steps. The glass transition temperatures were taken as the peak maximum of the loss modulus ( $E''$ ) curves measured at 1 Hz. All samples were heated twice in the DMA. After the first heat, the samples were allowed to slow cool in the DMA to provide matching thermal histories. All DMA results in this report were taken from second heat measurements.

---

## 4. Results and Discussion

---

Figures 2–7 illustrate the dynamic mechanical response of the thermal and e-beam-cured samples at constant frequency (1 Hz) as a function of temperature. The overall trends in the dynamic mechanical properties are similar between the thermal and e-beam curing routes. In both cases, as the molar ratio of 33% TMTE to DGEBF is increased, the  $T_g$  is elevated and the glass to rubber transition zone is broadened. The trifunctional TMTE increases the crosslink density ( $\rho_c$ ) of the cured IPN. An increase in the width of the distribution of segmental relaxation times is consistent with an increased  $\rho_c$  in highly crosslinked epoxy networks [3].

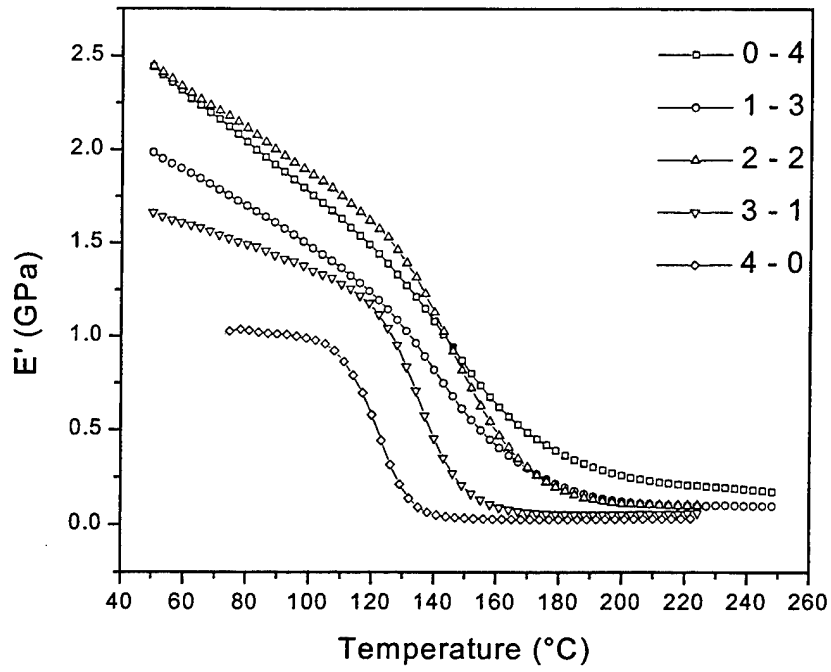


Figure 2. Storage modulus plots for thermal-cured IPNs.

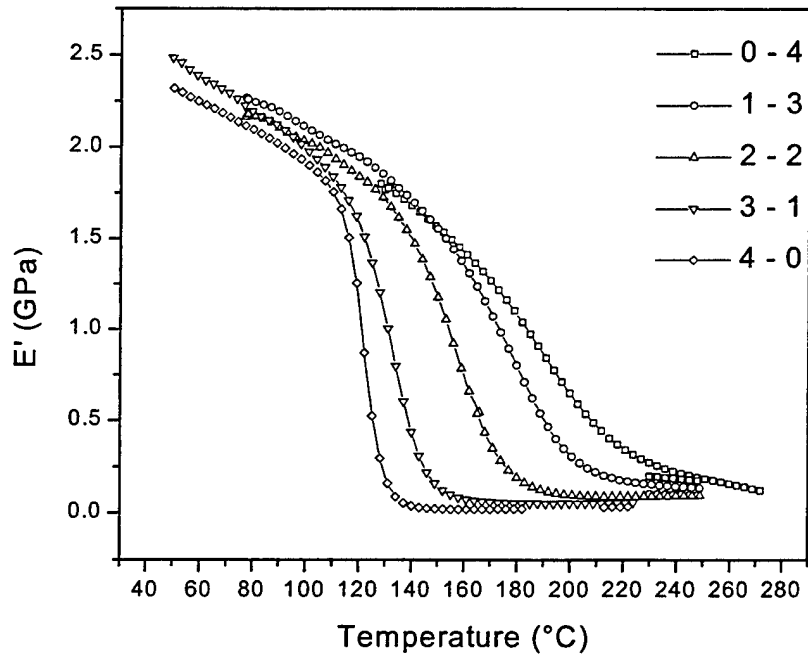


Figure 3. Storage modulus plots for e-beam-cured IPNs.

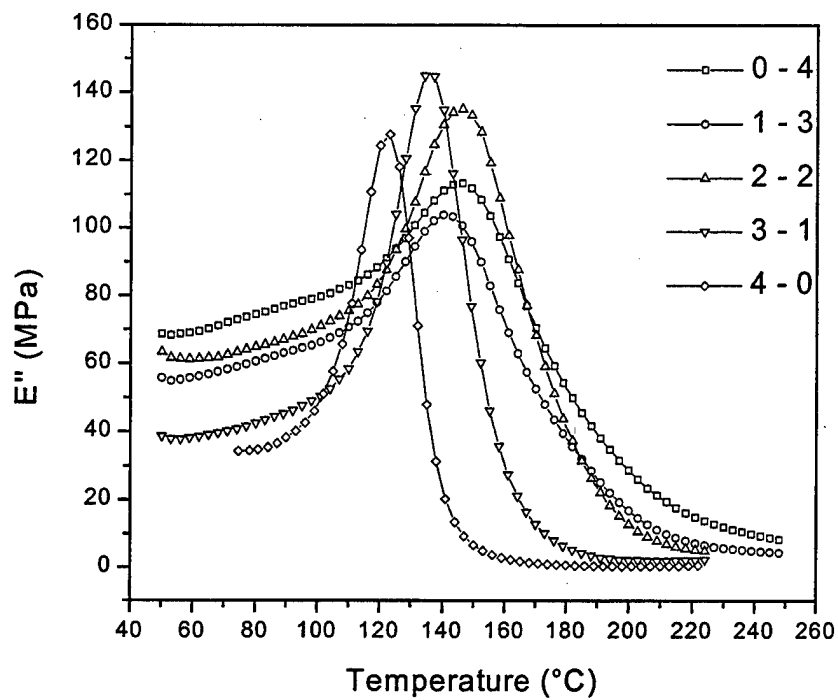


Figure 4. Loss modulus plots for thermal-cured IPNs.

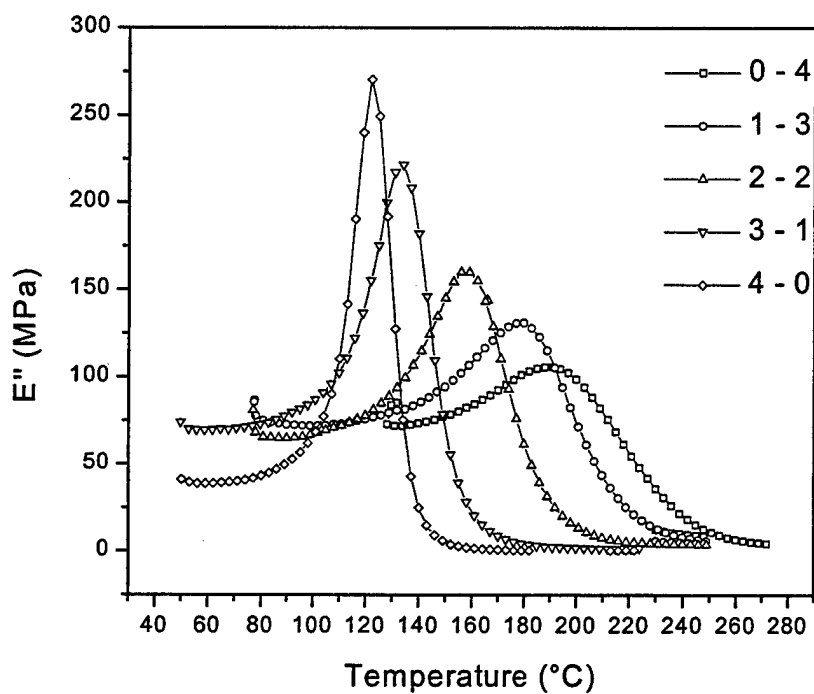


Figure 5. Loss modulus plots for e-beam-cured IPNs.

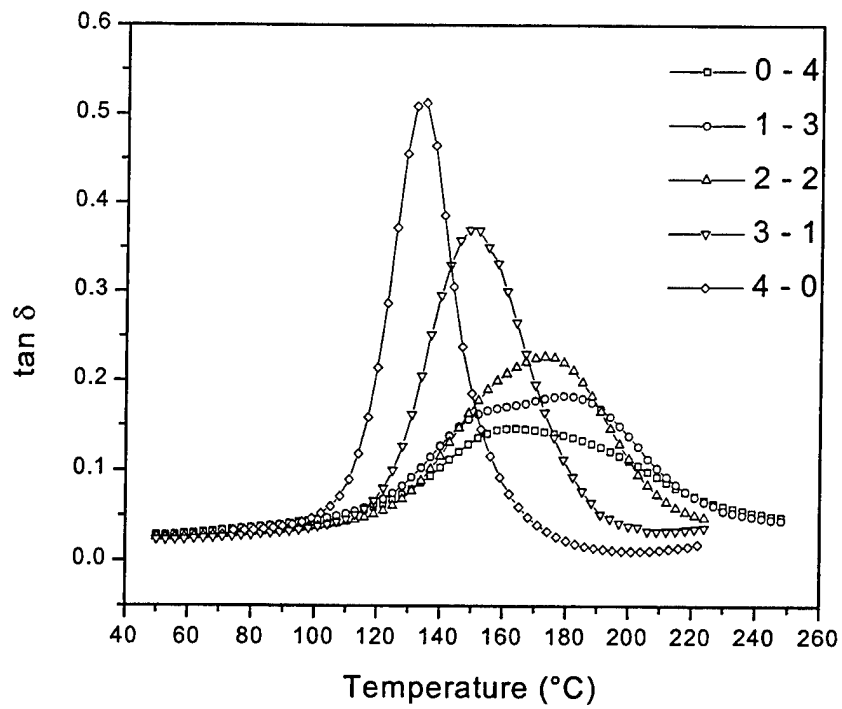


Figure 6. Loss tangent plots for thermal-cured IPNs.

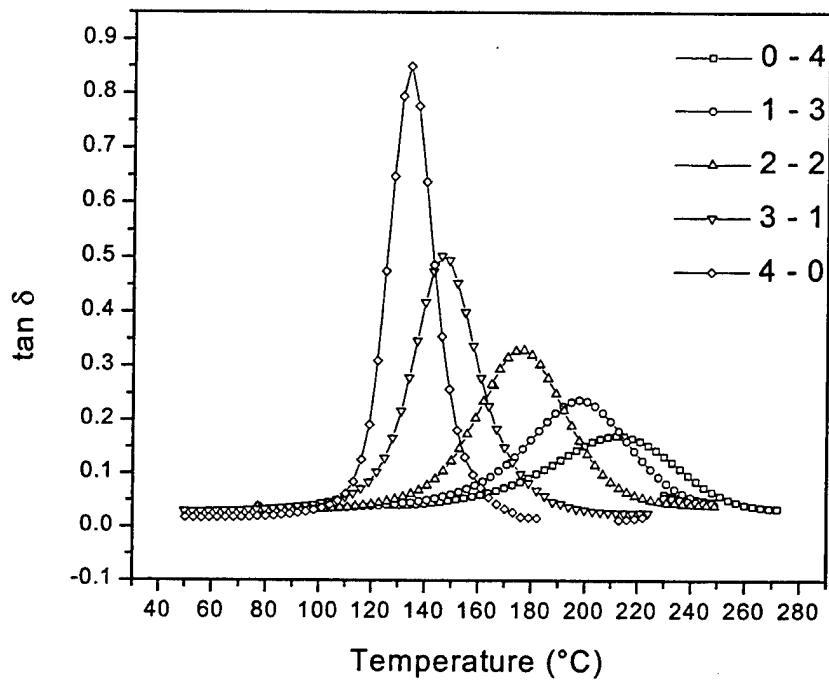


Figure 7. Loss tangent plots for e-beam-cured IPNs.

The 33% TMTE also covalently couples the epoxy-amine and free radical methacryl networks together, which increases the heterogeneity of molecular environments. This increase in  $T_g$  and breadth of the glass to rubber transition with increased coupling between the individual components of an IPN has been observed in other systems [4-7]. Akay and Rollins [4] determined that the broadening of the glass transition cannot be explained by a simple increase in crosslink density alone, and the coupling between the networks results in more complicated viscoelastic interactions. An apparent increase in crosslink density can be noticed in the rubbery regions of the storage modulus plots presented in Figures 2 and 3.

While the overall trends in the dynamic mechanical properties between the thermal- and e-beam-cured samples are similar, sufficient differences are present that merit further investigation. The e-beam-cured samples exhibit a steady rise in  $T_g$  from 122° to 190 °C, as seen in the  $E''$  and  $\tan \delta$  plots, as the molar ratio of the TMTE coupler is extended through the 4-0 to 0-4 samples, respectively. The  $T_g$  for the 4-0 (no coupler) thermal-cured samples is nearly identical to the e-beam counterpart at 123 °C, but the  $T_g$  values for the thermal route plateau at 145 °C beginning with the 2-2 sample. Fourier transform infrared (FTIR) results (not shown) indicate that the e-beam cure method achieves a greater degree of methacryl conversion than the thermal route, which results in the increased crosslink density and  $T_g$  for the e-beam-cured samples [2]. The depressed thermal conversion of methacryl functional groups is presumably due to the free radical propagation becoming restricted because of diminished molecular mobility as the thermal cure is advanced. It is interesting to note that the ultimate  $T_g$  reached during thermal cure of 145 °C closely matches the median thermal cure step of 140 °C. The thermal post-cure step at 250 °C increases the degree of methacryl conversion from 75-79% to 84-89%, but does not yield a further increase  $T_g$ . The e-beam-cured samples have a higher degree of methacryl conversion prior to post-curing (91-94%) and the additional post-cure step only increases the methacryl conversion by 2-4%.

The differences in glassy behavior between the thermal- and e-beam-cured IPNs are readily apparent as seen in Figures 2 and 3, respectively. The glassy storage moduli of the thermal-cured IPN vary greatly and rise from 1 GPa for the 4-0 sample to 2.5 GPa for the 0-4 sample. The glassy storage modulus of the e-beam-cured samples lies near 2.5 GPa for all of the samples regardless of the DGEBA to TMTE molar ratio. These results were also reproduced using another DMA [2], which adds weight to the argument that the differences in glassy response between the curing routes are real, and not instrument artifacts. Mobility in the glassy state is related to sub- $T_g$  local secondary relaxation mechanisms such as the  $\beta$  transition [8]. The secondary  $\beta$  transition in epoxies based upon common diglycidylether of bisphenol A (DGEBA) is centered near -60 °C and is caused by

motion of the hydroxypropylether linkage and phenol ring flips [9]. The amplitude of the damping peak caused by the  $\beta$  transition has been found to be inversely proportional to the crosslink density at ambient temperatures in traditional microstructure networks, which results in a decreased glassy modulus [10-13]. A possible explanation proposed for this effect is that a crosslink point isolates short segments of network chain, therefore uncoupling local motion from other neighboring chain segments [11]. It has also been postulated that decreasing the cross-link density will decrease the glassy modulus due to weaker Van der Waals interactions [14]. The results obtained for this research point towards the uncommon trend in that the thermal-cured IPNs with the lowest  $\rho_c$  (4-0 sample with 84% methacryl conversion) have the lowest magnitudes of glassy modulus. The e-beam-cured IPNs all have similar methacryl conversions of 95-97% and similar glassy moduli. The thermal- and e-beam-cured IPNs have identical thermal histories after the post-cure step, so it is difficult to gauge the cause of the modulus differences (free volume, degree of conversion, IPN microstructure, etc.) without performing a detailed analysis of the  $\beta$  transition. On the basis of differences in glassy modulus between the e-beam and thermal-cured IPNs, one could also expect interesting differences in the sub- $T_g$  nonequilibrium behavior [15]. This could lead to variations in the physical-aging rates between the e-beam and thermal-cured IPNs.

In addition to the differences in glassy modulus between the thermal- and e-beam-cured samples, significant changes in the  $\tan \delta$  peak in the glass transition region are also apparent. Figures 6 and 7 illustrate the  $\tan \delta$  plots as a function of DGEBF to TMTE molar ratio for the thermal- and e-beam-cured samples, respectively. The e-beam-cured sample displays a continuous shift in  $T_g$  towards higher temperatures with a corresponding broadening of peak width as the amount of TMTE is increased. The  $\tan \delta$  curves for the e-beam samples are also relatively symmetric and are absent of any shoulders. As mentioned previously, the  $T_g$  of the thermal-cured 0-4, 1-3, and 2-2 samples plateau near 145 °C due to diffusion considerations. Shoulders in the  $\tan \delta$  signals of the thermal-cured 1-3 and 0-4 samples also appear that are not evident in the corresponding e-beam samples. The observation of a shoulder or second peak in the DMA spectra of an IPN is caused by multiple molecular relaxation mechanisms of multiple phase domains [5, 16].

However, it is difficult to ascertain the molecular origin of the relaxation mechanism responsible for the  $\tan \delta$  shoulders present in the thermal-cured 1-3 and 0-4 samples from the simple isochronal DMA measurements performed for Figure 6. An alternative approach to enhance the shoulder region of the  $\tan \delta$  peaks is to sweep the frequency ( $f$ ) of the DMA measurement at isothermal temperatures. This method has been used successfully to separate the overlapping  $\beta$ -transition of an epoxy matrix from the low temperature  $\alpha$ -transition of an included rubber toughener [17]. The peak-shoulder separation

achieved during this type of frequency sweep is improved for overlapping molecular processes that differ greatly in Arrhenius activation energy ( $E_a$ ), as described by equation (1):

$$\ln\left(\frac{f}{f_o}\right) = -\frac{E_a}{R}\left(\frac{1}{T} - \frac{1}{T_o}\right), \quad (1)$$

where

$T$  = the temperature (in degrees Kelvin) of the peak maximum, and  
 $T_o$  = the reference temperature.

Figures 8 and 9 show the isothermal frequency sweep  $E''$  and  $\tan \delta$  plots for the e-beam-cured 1-3 sample, respectively. Again the e-beam-cured 1-3 sample displays a single homogeneous transition with no shoulders. The  $E''$  peaks range in temperature from approximately 170° to 190 °C as the frequency of the measurement is swept from 0.1 to 30 Hz, respectively. The corresponding  $\tan \delta$  signal peaks are roughly 20 °C greater than the loss modulus peaks.

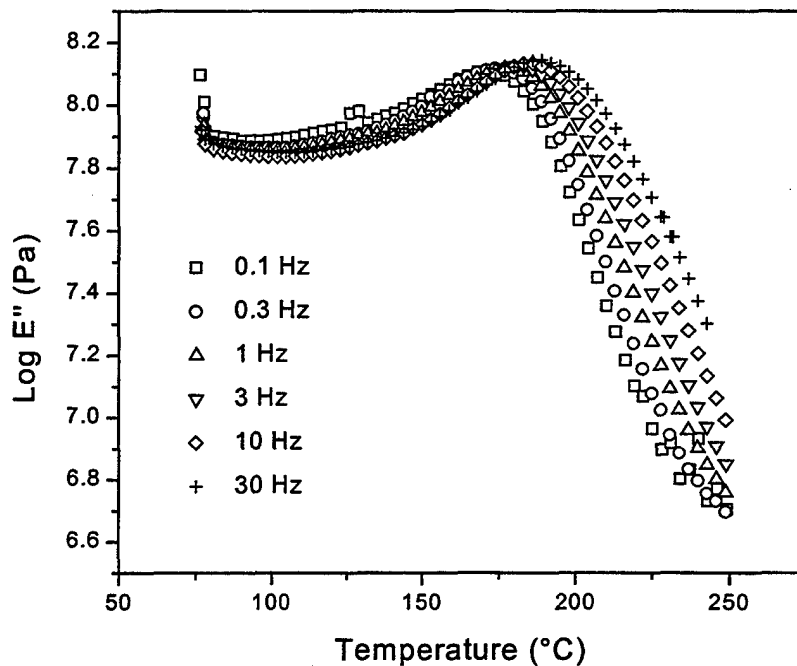


Figure 8. Loss modulus frequency sweep measurements of e-beam-cured 1-3 sample.

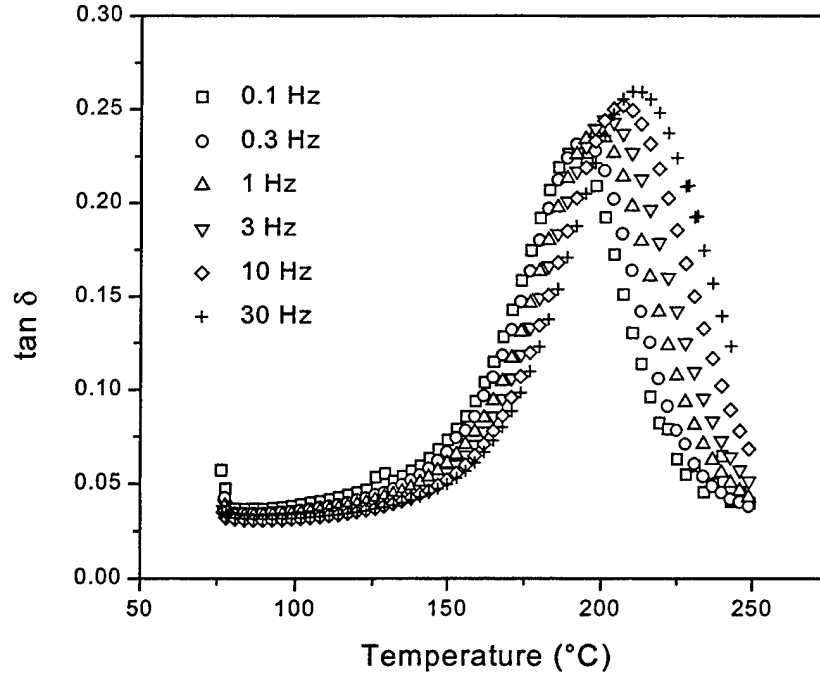


Figure 9. Loss tangent frequency sweep measurements of e-beam-cured 1-3 sample.

In contrast to the e-beam-cured 1-3 sample,  $E''$  shoulders are still evident in the multiple frequency-sweep plots of the thermal-cured 1-3 sample (Figure 10) at high temperatures trailing the peak maxima ( $\sim 190^{\circ}$ - $210^{\circ}$  °C), but are not shifted from the main loss modulus peaks at any measured frequency. Therefore, the molecular mechanism responsible for the loss modulus shoulder in the thermal case must have an Arrhenius activation energy nearly identical to the primarily observed transition. Furthermore, when the loss modulus curves of Figure 10 and the  $\tan \delta$  curves of Figure 11 are directly compared, an interesting observation is noted. The primary transition present in the  $E''$  curves ( $\sim 135^{\circ}$ - $155^{\circ}$  °C) correlate to the leading shoulders in the respective  $\tan \delta$  curves. The trailing shoulders in the  $E''$  curves ( $\sim 190^{\circ}$ - $210^{\circ}$  °C) link to the primary peaks in the  $\tan \delta$  curves. The difference in temperature between analogous  $E''$  and  $\tan \delta$  peaks for the thermal-cured 1-3 samples is nearly 40 °C. This raises more suspicion that the observed relaxations near 140°-145 °C for the higher crosslink density thermal samples are due to memory retention of the median oven-cure stage.

Cure memory in the dynamic mechanical glass transition has been observed in polyamidoamine-epoxy networks by other researchers [18]. Sanz et al. [19] also observed shoulders in the  $\tan \delta$  signals of stoichiometric epoxy-amine systems with temperatures and magnitudes dependent upon the thermal-cure conditions. This is a result of a fraction of the network structure attaining a high-crosslink density during gelation at the median-cure stage. During the post-cure stage,

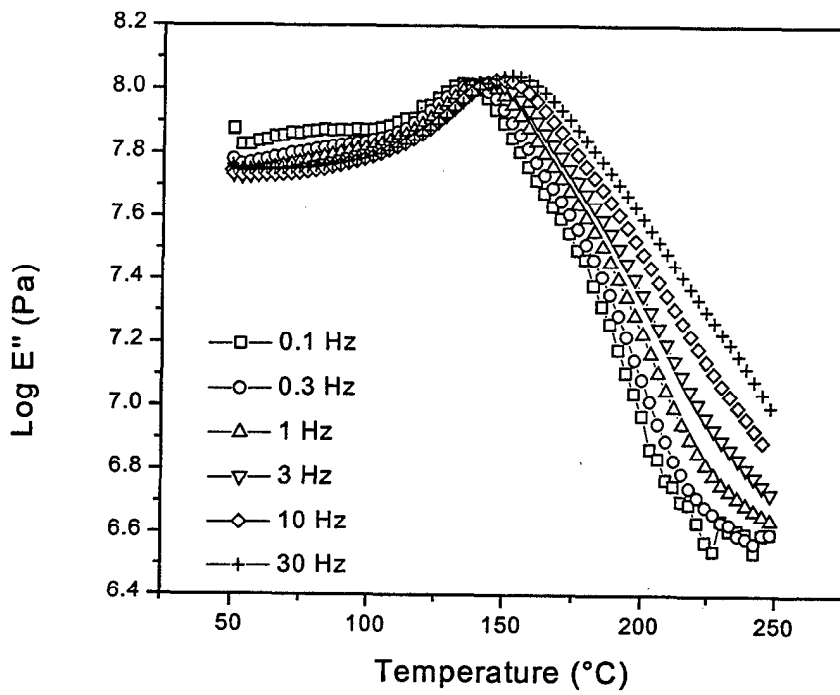


Figure 10. Loss modulus frequency sweep measurements of thermal-cured 1-3 sample.

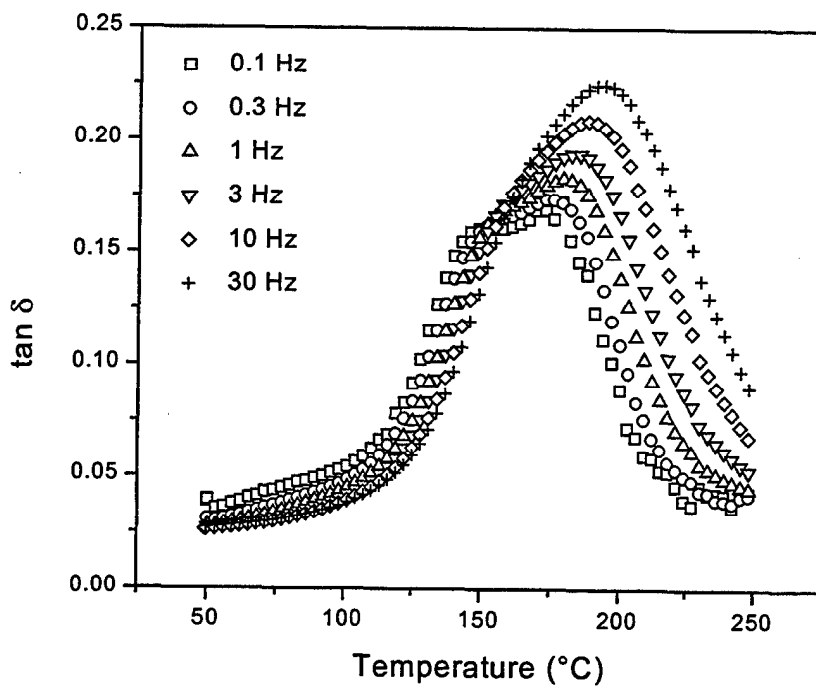


Figure 11. Loss tangent frequency sweep measurements of thermal-cured 1-3 sample.

further crosslinking reactions occur, but are diffusion limited within these regions of high-crosslink density from the previous cure stage. The physical heterogeneity between these regions of low- and high-crosslink density results in the broadness observed in the  $E''$  curves during DMA experiments. The broadness in the  $E''$  curves for the thermal-cured IPNs appears to be caused by physical mechanisms. In the case of the thermal-cured 1-3 samples, the  $E_a$  calculated from the primary loss modulus peaks (135°-155 °C range) is 477 kJ/mol and 456 kJ/mol from the  $\tan \delta$  peaks (175°-195 °C range). These values are very close to  $E_a$  values of 498 kJ/mol and 509 kJ/mol calculated for the e-beam 1-3  $E''$  and  $\tan \delta$  signals, respectively.

A goal of this research was to investigate the possibility of using DMA to correlate the observed densities and cure shrinkage of the IPN adhesives to free volume. Gerard et al. [20] have used this approach to relate the crosslink density and chain flexibility of model epoxy-amine networks to free volume. Akay and Rollins [4] also examined the free-volume and glass-transition broadening of polyurethane/poly (methyl methacrylate) IPNs from viscoelastic standpoint. For this research, the viscoelastic interpretations were derived from a similar perspective using master curves of the loss modulus, which were constructed in the frequency ( $\omega$ ) domain in the glass transition region ( $T_g \pm 30$  °C) following the time-temperature superposition principle (tTsp) [3]. Prior to shifting the modulus isotherms horizontally along the frequency axis, a vertical shift factor correction of  $T_o/T$  was applied, where  $T_o$  represents the reference temperature. The horizontal shift factors ( $a_T > T_g$ ) were then fitted to the empirical and free volume derived Williams-Landel/Ferry (WLF) equation (2). The WLF equation is used to describe the temperature dependence of the distribution of relaxation times ( $\tau$ ) in viscoelastic materials. The  $C_1$  and  $C_2$  constants of the WLF equation were determined using a nonlinear least squares fit. The fractional free volume at the glass transition ( $f_g$ ) and coefficient of thermal expansion of the fractional free volume ( $\alpha_f$ ) were then solved using the  $C_1$  and  $C_2$  constants and setting empirical Doolittle constant (B) equal to 1 [20, 21]. The  $C_1$  and  $C_2$  constants of the WLF equation can also be used to solve for  $E_a$ . The breadth of the distribution of relaxation times was quantified by fitting the master curves to the Kohlrausch-Williams/Watts (KWW) equation (5) and determining the coupling parameters ( $\beta$ ) [22]. The  $\beta$  parameters were found using the methodology outlined by Weiss et al. [23, 24].

$$\log a_T = \log \frac{\tau^*}{\tau_o^*} = \frac{-C_1(T - T_o)}{C_2 + (T - T_o)} \quad (2)$$

$$C_1 = \frac{B}{2.3f_g} ; C_2 = \frac{f_g}{\alpha_f} \quad (3)$$

$$E_a = -2.303RT^2 \frac{d \log a_T}{dT} \quad (4)$$

$$\phi(t) = \exp \left[ - \left( \frac{t}{\tau} \right)^\beta \right] \rightarrow 0 < \beta \leq 1 \quad (5)$$

Figures 12 and 13 show the  $E''$  master curves and KWW fits for the thermal and e-beam-cured samples, respectively. For each sample, the isotherms successfully shifted to form smooth and continuous master curves. The KWW equation also provided reasonable descriptions of the master curves, with the  $\beta$  parameters summarized in Table 1. For each cure route, it can be seen that the breadth of the  $E''$  master curves with increased TMTE concentration. This increase in coupling between networks and subsequent increase in crosslink density is reflected as a decrease in the  $\beta$  parameters (0.237 for the e-beam 4-0 sample to 0.113 for the e-beam 0-4 sample and 0.202 for the thermal 4-0 sample to 0.113 to the 0-4 thermal sample). The reference relaxation time used for the KWW fits is also provided.

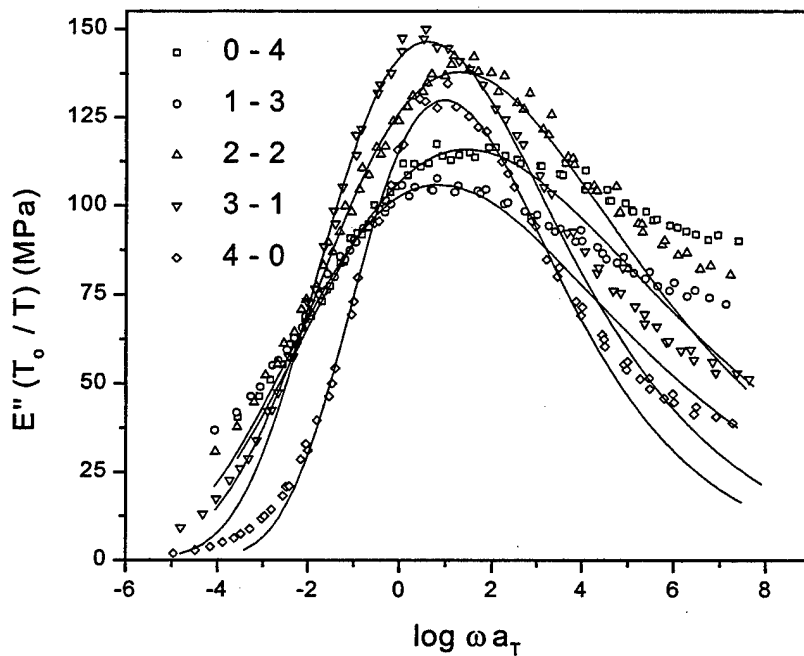


Figure 12. Loss modulus  $E''$  master curves and KWW fits for thermal-cured samples.

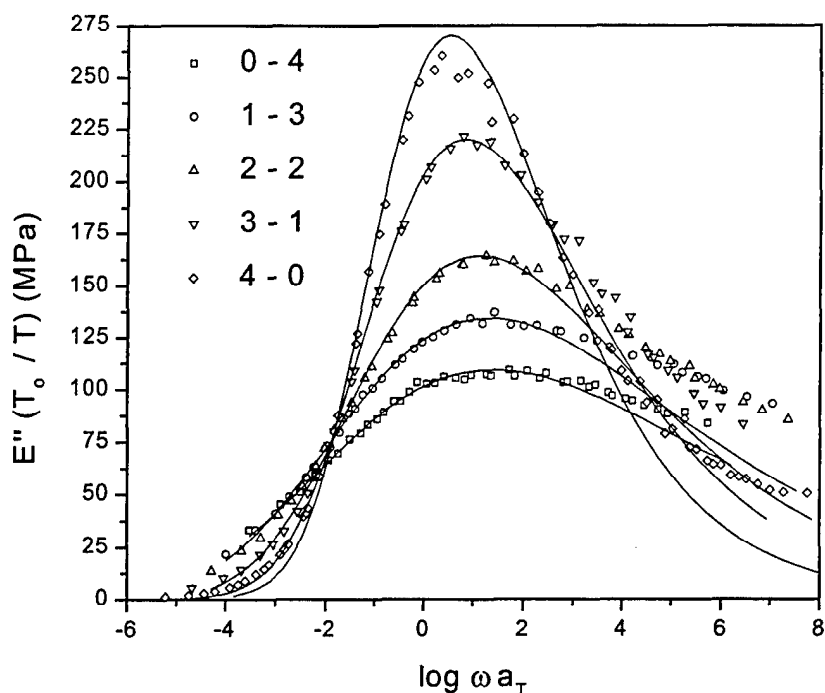


Figure 13.  $E''$  master curves and KWW fits for e-beam-cured samples.

However, for  $tT_{sp}$  to be gauged a success, the shift factor plots and WLF parameters must also be considered. Table 1 also summarizes  $T_g$ ,  $E_a$ ,  $C_1$ ,  $C_2$ ,  $f_g$ , and  $\alpha_f$ . Figures 14 and 15 show the shift factor plots for the thermal and e-beam-cured samples, respectively. The values calculated for the thermal-cured 0-4, 1-3, and 2-2 samples must certainly be incorrect as multiple relaxation processes were clearly observed in the  $E''$  and  $\tan \delta$  signals [3]. This can also be seen in the shift factor plots (Figure 14), as the curves for these samples were nearly linear and deviated from WLF behavior. The thermal-cured 2-2 sample fits the WLF equation so poorly that none of the parameters could be reasonably determined or approximated. The WLF parameters obtained for the thermal-cured samples with little inter-network coupling, 4-0 and 3-1, seemed reasonable.

The most interesting viscoelastic behavior is observed in the e-beam-cured IPN where no directly observable multiple relaxation peaks or shoulders were found in the  $E''$  and  $\tan \delta$  signals. The shift factor plots for the e-beam-curing process (Figure 15) are similar to the thermal-cured counterparts in that as the molar ratio of TMTE coupler to DGEBA is increased, the temperature sensitivity of  $\log a_T$  decreases. This result is consistent with the results of Ogata et al. [25], where a decrease in the temperature and frequency dependency of the glass to rubber relaxation for phenol-formaldehyde novolac epoxy networks was found as the crosslink density was increased. Significant departures from typical epoxy-amine network properties are found in the values of  $f_g$  and  $\alpha_f$  calculated for the e-beam-cured IPNs. The uncoupled 4-0 sample has values of  $f_g$  and  $\alpha_f$  that are in the range

Table 1. Viscoelastic parameters derived from fits of master curves.

Sample	$\beta \times 10^1$	$\tau \times 10^2$ (s)	$T_g$ (°C)	$E_a^a$ (kJ/mol)	$E_a^b$ (kJ/mol)	$C_1$	$C_2$ (°C)	$f_g \times 10^2$	$\alpha_f \times 10^4$ (°C <sup>-1</sup> )
E-beam									
0-4 E	1.13	0.38	190	472.2	484.4	47.1	399.1	0.92	2.3
1-3 E	1.25	0.48	181	497.0	623.6	19.8	125.3	2.2	1.8
2-2 E	1.53	0.75	158	627.5	642.3	17.1	94.7	2.5	2.7
3-1 E	1.92	1.4	134	597.7	710.2	13.3	59.4	3.3	5.5
4-0 E	2.37	2.9	122	631.9	902.8	11.0	36.4	4.0	10.6
Thermal									
0-4 T <sup>c</sup>	1.15	0.35	145	440.4	443.9	22.9	172.6	1.9	1.1
1-3 T <sup>c</sup>	1.25	1.4	141	477.3	614.0	11.9	63.6	3.7	5.7
2-2 T <sup>c</sup>	1.31	0.5	145	501.4	c	c	c	c	c
3-1 T	1.70	2.5	135	659.6	709.4	14.8	66.5	2.9	4.4
4-0 T	2.02	1.1	123	623.1	699.8	14.8	63.5	2.9	4.6

<sup>a</sup>Arrhenius.

<sup>b</sup>WLF.

<sup>c</sup>Multiple transitions observed in loss modulus spectra.

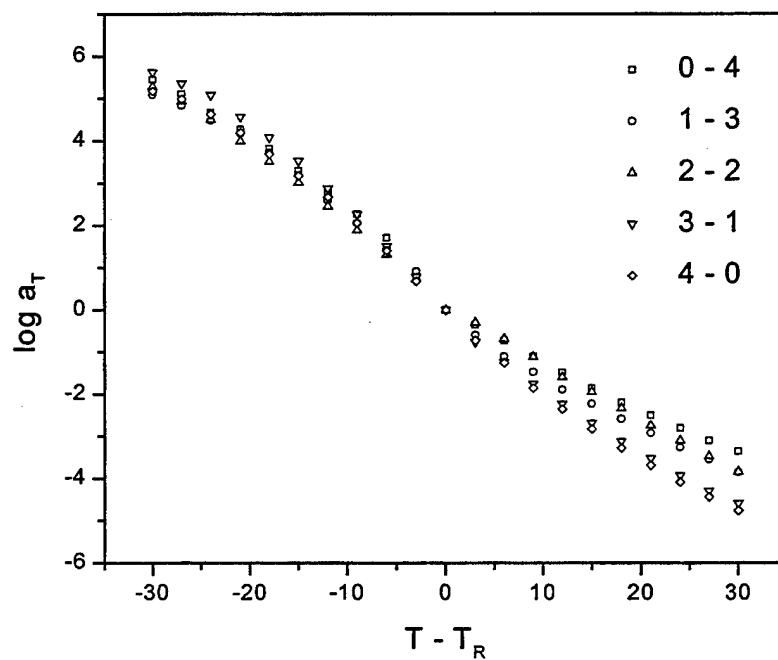


Figure 14. Shift factor plots for thermal-cured IPNs.

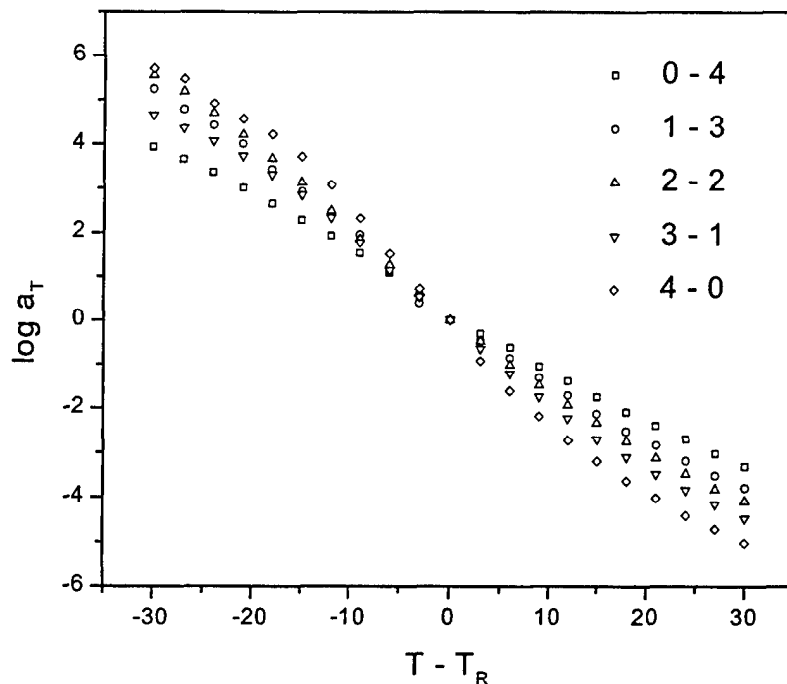


Figure 15. Shift factor plots for e-beam-cured IPNs.

of values for conventional thermosets, as determined by Gerard et al. [20]. As the molar ratio of TMTE to DGEBA is increased, the calculated values of  $f_g$  and  $\alpha_f$  decrease significantly. The most coupled sample (0-4) has an  $\alpha_f$  value in the rubbery region, which is an order of magnitude lower than the typical values reported by Gerard. This inter-network coupling profoundly increases the overall crosslink density of the IPN. One must also keep in mind that the viscoelastic response of the highly coupled e-beam IPN samples also deviates considerably from ideal WLF behavior, so the assumption of a single relaxation mechanism may not be valid. While it is uncertain whether or not multiple relaxation mechanisms from a heterogeneously crosslinked network structure are active in the case of the e-beam-cured IPNs, the trends in the viscoelastic data point towards a more homogeneously crosslinked network in comparison to the thermal-cure counterpart.

---

## 5. References

---

1. Sperling, L. H. *Interpenetrating Polymer Networks and Related Materials*. New York: Plenum Publishing, 1981.
2. Dalal, U. P., and G. R. Palmese. "Formation of In-Situ Sequential Interpenetrating Polymer Networks via Thermal and Radiation Curing." CCM Report 99-14, University of Delaware, Center for Composite Materials, Newark, DE, 1999.
3. Ferry, J. D. *Viscoelastic Properties of Polymers*. 2nd Edition, New York: John Wiley & Sons, 1970.
4. Akay, M., and S. N. Rollins. "Transition Broadening and WLF Relationship in Polyurethane/Poly(methyl methacrylate) Interpenetrating Polymer Networks." *Polymer*, vol. 34, pp. 967-971, 1993.
5. Chen, C. H., J. W. Chen, M. H. Chen, and Y. M. Li. "Simultaneous Full-Interpenetrating Polymer Networks of Blocked Polyurethane and Vinyl Ester. II. Static and Dynamic Mechanical Properties." *Journal of Applied Polymer Science*, vol. 71, pp. 1977-1985, 1999.
6. Nair, C. P. R., T. Francis, T. M. Vijayan, and K. Krishnan. "Sequential Interpenetrating Polymer Networks from Bisphenol A Based Cyanate Ester and Bismaleimide: Properties of the Neat Resin and Composites." *Journal of Applied Polymer Science*, vol. 74, pp. 2737-2746, 1999.
7. Han, J. L., and K. Y. Li. "Graft Interpenetrating Polymer Networks of Bismaleimide and Epoxy Based on Maleimide-Terminated Polyurethane-Grafted Epoxy." *Polymer*, vol. 31, pp. 401-405, 1999.
8. Fitz, B., S. Andjelic, and J. Mijovic. "Reorientational Dynamics and Intermolecular Cooperativity of Reactive Polymers. 1. Model Epoxy-Amine Systems." *Macromolecules*, vol. 30, pp. 5227-5238, 1999.
9. Bershtein, V. A., N. N. Peschanskaya, J. L. Halary, and L. Monnerie. "The Sub-T<sub>g</sub> Relaxations in Pure and Antiplasticized Model Epoxy Networks as Studied by High Resolution Creep Rate Spectroscopy." *Polymer*, vol. 40, pp. 6687-6698, 1999.
10. Cukierman, S., J. L. Halary, and L. Monnerie. "Dynamic Mechanical Response of Model Epoxy Networks in the Glassy State." *Polymer Engineering and Science*, vol. 31, pp. 1476-1482, 1991.
11. Verdu, J., and A. Tcharkhtchi. "Elastic Properties of Thermosets in Glassy State." *Die Angewandte Makromolekulare Chemie*, vol. 240, pp. 31-38, 1996.

12. Georjon, O., G. Schwach, J. F. Gerard, and J. Galy. "Molecular Mobility in Polycyanurate Networks Investigated by Viscoelastic Measurements and Molecular Simulations." *Polymer Engineering and Science*, vol. 37, pp. 1606-1620, 1997.
13. Urbaczewski-Espuche, E., J. Galy, J. F. Gerard, J. P. Pascault, and H. Sautereau. "Influence of Chain Flexibility and Crosslink Density on Mechanical Properties of Epoxy/Amine Networks." *Polymer Engineering and Science*, vol. 31, pp. 1572-1580, 1991.
14. Sindt, O., J. Perez, and J. F. Gerard. "Molecular Architecture-Mechanical Behaviour Relationships in Epoxy Networks." *Polymer*, vol. 37, pp. 2989-2997, 1996.
15. Tant, M. R., and G. L. Wilkes. "An Overview of the Nonequilibrium Behavior of Polymer Glasses." *Polymer Engineering and Science*, vol. 21, pp. 874-895, 1981.
16. Kim, Y. S., H. S. Min, W. J. Choi, and S. C. Kim. "Dynamic Mechanical Modeling of PEI/Dicyanate Semi-IPNs." *Polymer Engineering and Science*, vol. 40, pp. 665-675, 2000.
17. Sands, J. M., R. E. Jensen, B. K. Fink, and S. H. McKnight. "Synthesis of Elastomer-Modified Epoxy-Methacrylate Sequential Interpenetrating Networks." *Journal of Applied Polymer Science*, vol. 81, pp. 530-545, 2001.
18. Lian, M. K. "Study of Durability in Epoxy Bonded Joints in Aqueous Environments." Masters thesis, Virginia Polytechnic Institute and State University, Blacksburg, VA, 1998.
19. Sanz, G., J. Garmendia, M. A. Andres, and I. Mondragon. "Dependence of Dynamic Mechanical Behavior of DGEBA/DDM Stoichiometric Epoxy Systems on the Conditions of Curing Process." *Journal of Applied Polymer Science*, vol. 55, pp. 75-87, 1995.
20. Gerard, J. F., J. Galy, and J. P. Pascault. "Viscoelastic Response of Model Epoxy Networks in the Glass Transition Region." *Polymer Engineering and Science*, vol. 31, pp. 615-621, 1991.
21. Doolittle, A. K., and D. B. Doolittle. *Journal of Applied Physics*, vol. 28, pp. 901-905, 1957.
22. Cook, M., G. Williams, and D. C. Watts. "Correlation Function Approach to the Dielectric Behaviour of Amorphous Polymers." *Transactions of the Faraday Society*, vol. 66, pp. 2503-2511, 1970.
23. Weiss, G. H., J. T. Bendler, and M. Dishon. "Analysis of Dielectric Loss Data Using the Williams-Watts Function." *Journal of Chemical Physics*, vol. 83, pp. 1424-1427, 1985.

24. Weiss, G. H., M. Dishon, A. M. Long, J. T. Bendler, A. A. Jones, P. T. Inglefield, and A. Bandis. "Improved Computational Methods for the Calculation of the Kohlrausch-Williams/Watts (KWW) Decay Functions." *Polymer*, vol. 35, pp. 1880-1883, 1994.
25. Ogata, M., N. Kinjo, and T. Kawata. "Effects of Crosslinking on Physical Properties of Phenol-Formaldehyde Novolac Cured Epoxy Resins." *Journal of Applied Polymer Science*, vol. 48, pp. 583-601, 1993.

INTENTIONALLY LEFT BLANK.

---

## List of Acronyms and Abbreviations

---

$a_T$	WLF isothermal shift factor
B	Doolittle equation parameter
$\beta$ parameter	KWW equation fitting parameter
$\beta$ transition	localized glassy polymeric sub- $T_g$ relaxation
$^{\circ}\text{C}$	degrees Celcius
$C_1$	WLF fitting parameter
$C_2$	WLF fitting parameter
DGEBA	diglycidyl ether of bisphenol A
DGEBF	diglycidyl ether of bisphenol F epoxy resin
DMA	dynamic mechanical analysis
$E'$	dynamic storage modulus
$E''$	dynamic loss modulus
$E_a$	Arrhenius activation energy
e-beam	electron beam
EEW	epoxy equivalent weight
$f_g$	fractional free volume at $T = T_g$
FTIR	Fourier transform infrared spectroscopy
GPa	giga Pascals
HDDMA	1,6-hexanediol dimethacrylate
IPN	interpenetrating polymer network
KWW	Kohlrausch-William/Watts equation
mm	millimeters
MPa	mega Pascals
PACM	bis (p-aminocyclohexyl) methane
T	temperature
$T_g$	glass transition temperature
$T_0$	WLF equation reference temperature
$\tan \delta$	$E''/E'$

$tT_{sp}$	time-temperature superposition principle
TMTE	triphenylmethane triglycidyl ether
WLF	Williams-Landel/Ferry equation
4-0	4 mols of DGEBF epoxy to 0 mols of 33% TMTE
3-1	3 mols of DGEBF epoxy to 1 mols of 33% TMTE
2-2	2 mols of DGEBF epoxy to 2 mols of 33% TMTE
1-3	1 mols of DGEBF epoxy to 3 mols of 33% TMTE
0-4	0 mols of DGEBF epoxy to 4 mols of 33% TMTE
$\alpha_f$	coefficient of thermal expansion of the fractional free volume
$\mu\text{m}$	micrometers
$\omega$	angular frequency
$\rho_c$	crosslink density
$\tau$	relaxation time constant of KWW equation

<u>NO. OF COPIES</u>	<u>ORGANIZATION</u>
2	DEFENSE TECHNICAL INFORMATION CENTER DTIC OCA 8725 JOHN J KINGMAN RD STE 0944 FT BELVOIR VA 22060-6218
1	HQDA DAMO FDT 400 ARMY PENTAGON WASHINGTON DC 20310-0460
1	OSD OUSD(A&T)/ODDR&E(R) DR R J TREW 3800 DEFENSE PENTAGON WASHINGTON DC 20301-3800
1	COMMANDING GENERAL US ARMY MATERIEL CMD AMCRDA TF 5001 EISENHOWER AVE ALEXANDRIA VA 22333-0001
1	INST FOR ADVNCD TCHNLGY THE UNIV OF TEXAS AT AUSTIN 3925 W BRAKER LN STE 400 AUSTIN TX 78759-5316
1	US MILITARY ACADEMY MATH SCI CTR EXCELLENCE MADN MATH THAYER HALL WEST POINT NY 10996-1786
1	DIRECTOR US ARMY RESEARCH LAB AMSRL D DR D SMITH 2800 POWDER MILL RD ADELPHI MD 20783-1197
1	DIRECTOR US ARMY RESEARCH LAB AMSRL CI AI R 2800 POWDER MILL RD ADELPHI MD 20783-1197

<u>NO. OF COPIES</u>	<u>ORGANIZATION</u>
3	DIRECTOR US ARMY RESEARCH LAB AMSRL CI LL 2800 POWDER MILL RD ADELPHI MD 20783-1197
3	DIRECTOR US ARMY RESEARCH LAB AMSRL CI IS T 2800 POWDER MILL RD ADELPHI MD 20783-1197
	<u>ABERDEEN PROVING GROUND</u>
2	DIR USARL AMSRL CI LP (BLDG 305)

<u>NO. OF COPIES</u>	<u>ORGANIZATION</u>
1	DIRECTOR US ARMY RESEARCH LAB AMSRL CP CA D SNIDER 2800 POWDER MILL RD ADELPHI MD 20783-1145
1	DIRECTOR US ARMY RESEARCH LAB AMSRL CI IS R 2800 POWDER MILL RD ADELPHI MD 20783-1145
3	DIRECTOR US ARMY RESEARCH LAB AMSRL OP SD TL 2800 POWDER MILL RD ADELPHI MD 20783-1145
1	DPTY ASST SECY FOR R&T SARD TT THE PENTAGON RM 3EA79 WASHINGTON DC 20301-7100
1	COMMANDER US ARMY MATERIEL CMD AMXMI INT 5001 EISENHOWER AVE ALEXANDRIA VA 22333-0001
1	COMMANDER US ARMY ARDEC AMSTA AR WET T SACHAR BLDG 172 PICATINNY ARSENAL NJ 07806-5000
1	COMMANDER US ARMY ARDEC AMSTA AR WEA J BRESCIA PICATINNY ARSENAL NJ 07806-5000
1	COMMANDER US ARMY TACOM AMSTA SF WARREN MI 48397-5000

<u>NO. OF COPIES</u>	<u>ORGANIZATION</u>
2	COMMANDER US ARMY AMCOM AVIATION APPLIED TECH DIR J SCHUCK FT EUSTIS VA 23604-5577
5	COMMANDER US ARMY TACOM AMSTA JSK J FLORENCE AMSTA TR D D OSTBERG B RAJU AMSTA CS SF H HUTCHINSON F SCHWARZ WARREN MI 48397-5000
1	USA SBCCOM PM SOLDIER SPT AMSSB PM RSS A J CONNORS KANSAS ST NATICK MA 01760-5057
2	USA SBCCOM MATERIAL SCIENCE TEAM AMSSB RSS J HERBERT M SENNETT KANSAS ST NATICK MA 01760-5057
2	OFC OF NAVAL RESEARCH D SIEGEL CODE 351 J KELLY 800 N QUINCY ST ARLINGTON VA 22217-5660
1	NAVAL SURFACE WARFARE CTR TECH LIBRARY CODE 323 17320 DAHLGREN RD DAHLGREN VA 22448
1	COMMANDER US ARMY ARDEC AMSTA AR CCH P J LUTZ PICATINNY ARSENAL NJ 07806-5000

<u>NO. OF COPIES</u>	<u>ORGANIZATION</u>
8	DIRECTOR US ARMY NATIONAL GROUND INTELLIGENCE CTR D LEITER MS 404 M HOLTUS MS 301 M WOLFE MS 307 S MINGLEDORF MS 504 J GASTON MS 301 W GSTATTENBAUER MS 304 R WARNER MS 305 J CRIDER MS 306 220 SEVENTH ST NE CHARLOTTESVILLE VA 22091
8	US ARMY SBCCOM SOLDIER SYSTEMS CENTER BALLISTICS TEAM J WARD W ZUKAS P CUNNIFF J SONG MARINE CORPS TEAM J MACKIEWICZ BUS AREA ADVOCACY TEAM W HASKELL AMSSB RCP SS W NYKVIST S BEAUDOIN KANSAS ST NATICK MA 01760-5019
1	EXPEDITIONARY WARFARE DIV N85 F SHOUP 2000 NAVY PENTAGON WASHINGTON DC 20350-2000
7	US ARMY RESEARCH OFC A CROWSON H EVERETT J PRATER G ANDERSON D STEPP D KISEROW J CHANG PO BOX 12211 RESEARCH TRIANGLE PARK NC 27709-2211

<u>NO. OF COPIES</u>	<u>ORGANIZATION</u>
2	NAVAL SURFACE WARFARE CTR CARDEROCK DIVISION R CRANE CODE 2802 C WILLIAMS CODE 6553 3A LEGGETT CIR BETHESDA MD 20054-5000
2	AFRL F ABRAMS J BROWN BLDG 653 2977 P ST STE 6 WRIGHT PATTERSON AFB OH 45433-7739
1	OAK RIDGE NATIONAL LABORATORY C EBERLE MS 8048 PO BOX 2008 OAK RIDGE TN 37831
1	HYDROGEOLOGIC INC SERDP ESTCP SPT OFC S WALSH 1155 HERNDON PKWY STE 900 HERNDON VA 20170
3	NASA LANGLEY RSCH CTR AMSRL VS W ELBER MS 266 F BARTLETT JR MS 266 G FARLEY MS 266 HAMPTON VA 23681-0001
1	UDLP G THOMAS PO BOX 58123 SANTA CLARA CA 95052
2	UDLP R BRYNSVOLD P JANKE MS 170 4800 EAST RIVER RD MINNEAPOLIS MN 55421-1498

NO. OF  
COPIES ORGANIZATION

ABERDEEN PROVING GROUND

1 DIRECTOR  
US ARMY RESEARCH LAB  
AMSRL OP AP L  
APG MD 21005-5066

21 DIR USARL  
AMSRL CS IO FI  
M ADAMSON  
AMSRL WM  
J SMITH  
D VIECHNICKI  
G HAGNAUER  
J MCCAULEY  
AMSRL WM B  
A HORST  
AMSRL WM BD  
B FORCH  
AMSRL WM BF  
J LACETERA  
AMSRL WM MA  
L GHORSE  
S MCKNIGHT  
AMSRL WM MB  
B FINK  
T BOGETTI  
S GHORSE  
D GRANVILLE  
C HOPPEL  
J SANDS  
E WETZEL  
AMRSL WM MC  
J BEATTY  
AMSRL WM MD  
W ROY  
AMSRL WM RP  
C SHOEMAKER  
AMSRL WM T  
B BURNS

<u>NO. OF</u> <u>COPIES</u>	<u>ORGANIZATION</u>	<u>NO. OF</u> <u>COPIES</u>	<u>ORGANIZATION</u>
1	LTD R MARTIN MERL TAMWORTH RD HERTFORD SG13 7DG UK	1	ISRAEL INST OF TECHNOLOGY S BODNER FACULTY OF MECHANICAL ENGR HAIFA 3200 ISRAEL
1	SMC SCOTLAND P W LAY DERA ROSYTH ROSYTH ROYAL DOCKYARD DUNFERMLINE FIFE KY 11 2XR UK	1	DSTO WEAPONS SYSTEMS DIVISION N BURMAN RLLWS SALISBURY SOUTH AUSTRALIA 5108 AUSTRALIA
1	CIVIL AVIATION ADMINISTRATION T GOTTESMAN PO BOX 8 BEN GURION INTERNL AIRPORT LOD 70150 ISRAEL	1	ECOLE ROYAL MILITAIRE E CELENS AVE DE LA RENAISSANCE 30 1040 BRUXELLE BELGIQUE
1	AEROSPATIALE S ANDRE A BTE CC RTE MD132 316 ROUTE DE BAYONNE TOULOUSE 31060 FRANCE	1	DEF RES ESTABLISHMENT VALCARTIER A DUPUIS 2459 BOULEVARD PIE XI NORTH VALCARTIER QUEBEC CANADA PO BOX 8800 COURCELETTE GOA IRO QUEBEC CANADA
1	DRA FORT HALSTEAD P N JONES SEVEN OAKS KENT TN 147BP UK	1	INSTITUT FRANCO ALLEMAND DE RECHERCHES DE SAINT LOUIS DE M GIRAUD 5 RUE DU GENERAL CASSAGNOU BOITE POSTALE 34 F 68301 SAINT LOUIS CEDEX FRANCE
1	DEFENSE RESEARCH ESTAB VALCARTIER F LESAGE COURCELETTE QUEBEC COA IRO CANADA	1	ECOLE POLYTECH J MANSON DMX LTC CH 1015 LAUSANNE SWITZERLAND
1	SWISS FEDERAL ARMAMENTS WKS W LANZ ALLMENDSTRASSE 86 3602 THUN SWITZERLAND	1	TNO DEFENSE RESEARCH R IJSSELSTEIN ACCOUNT DIRECTOR R&D ARMEE PO BOX 6006 2600 JA DELFT THE NETHERLANDS
1	DYNAMEC RESEARCH AB AKE PERSSON BOX 201 SE 151 23 SODERTALJE SWEDEN		

<u>NO. OF COPIES</u>	<u>ORGANIZATION</u>
2	FOA NATL DEFENSE RESEARCH ESTAB DIR DEPT OF WEAPONS & PROTECTION B JANZON R HOLMLIN S 172 90 STOCKHOLM SWEDEN
2	DEFENSE TECH & PROC AGENCY GROUND I CREWTHIER GENERAL HERZOG HAUS 3602 THUN SWITZERLAND
1	MINISTRY OF DEFENCE RAFAEL ARMAMENT DEVELOPMENT AUTH M MAYSELESS PO BOX 2250 HAIFA 31021 ISRAEL
1	TNO DEFENSE RESEARCH I H PASMAN POSTBUS 6006 2600 JA DELFT THE NETHERLANDS
1	B HIRSCH TACHKEMONY ST 6 NETAMUA 42611 ISRAEL
1	DEUTSCHE AEROSPACE AG DYNAMICS SYSTEMS M HELD PO BOX 1340 D 86523 SCHROBENHAUSEN GERMANY

# REPORT DOCUMENTATION PAGE

*Form Approved  
OMB No. 0704-0188*

Public reporting burden for this collection of information is estimated to average 1 hour per response, including the time for reviewing instructions, searching existing data sources, gathering and maintaining the data needed, and completing and reviewing the collection of information. Send comments regarding this burden estimate or any other aspect of this collection of information, including suggestions for reducing this burden, to Washington Headquarters Services, Directorate for Information Operations and Reports, 1215 Jefferson Davis Highway, Suite 1204, Arlington, VA 22202-4302, and to the Office of Management and Budget, Paperwork Reduction Project(0704-0188), Washington, DC 20503.

<b>1. AGENCY USE ONLY (Leave blank)</b>		<b>2. REPORT DATE</b> March 2002	<b>3. REPORT TYPE AND DATES COVERED</b> Final, August 2000 – August 2001	
<b>4. TITLE AND SUBTITLE</b> Dynamic Mechanical Analysis of E-Beam and Thermally Curable IPN Thermosets			<b>5. FUNDING NUMBERS</b> AH42	
<b>6. AUTHOR(S)</b> Robert E. Jensen, Giuseppe R. Palmese,* and Steven H. McKnight				
<b>7. PERFORMING ORGANIZATION NAME(S) AND ADDRESS(ES)</b> U.S. Army Research Laboratory ATTN: AMSRL-WM-MA Aberdeen Proving Ground, MD 21005-5069			<b>8. PERFORMING ORGANIZATION REPORT NUMBER</b> ARL-TR-2698	
<b>9. SPONSORING/MONITORING AGENCY NAMES(S) AND ADDRESS(ES)</b>			<b>10. SPONSORING/MONITORING AGENCY REPORT NUMBER</b>	
<b>11. SUPPLEMENTARY NOTES</b> *Drexel University, Philadelphia, PA 19104				
<b>12a. DISTRIBUTION/AVAILABILITY STATEMENT</b> Approved for public release; distribution is unlimited.			<b>12b. DISTRIBUTION CODE</b>	
<b>13. ABSTRACT (Maximum 200 words)</b> Interpenetrating polymer network (IPN) materials possess unique properties that can be exploited for multicomponent composite armor systems, including toughness and thermal stability. E-beam curing of composites and adhesives offers advantages, such as reduced cure shrinkages, over traditional autoclave processing by curing multiple resins through the thickness for thick-section composites in a single step. Because of the complexity and thickness of composite integral armor structures, e-beam curing is an attractive processing method for Future Combat System applications, and the development of these new resins permits this approach. This research seeks to discern the differences in viscoelastic behavior between traditional thermal and e-beam curing in IPN resins, as these viscoelastic characteristics may prove important for composite integral armor applications.				
<b>14. SUBJECT TERMS</b> IPN, DMA, viscoelasticity, epoxy, methacryl			<b>15. NUMBER OF PAGES</b> 34	
			<b>16. PRICE CODE</b>	
<b>17. SECURITY CLASSIFICATION OF REPORT</b> UNCLASSIFIED	<b>18. SECURITY CLASSIFICATION OF THIS PAGE</b> UNCLASSIFIED	<b>19. SECURITY CLASSIFICATION OF ABSTRACT</b> UNCLASSIFIED	<b>20. LIMITATION OF ABSTRACT</b> UL	

INTENTIONALLY LEFT BLANK.